MATHEMATICAL BIOSCIENCES
AND ENGINEERING
Volume **10**, Number **1**, February **2013**

doi:10.3934/mbe.2013.10.167

pp. **167–184**

A STRUCTURAL MODEL OF THE VEGF SIGNALLING PATHWAY: EMERGENCE OF ROBUSTNESS AND REDUNDANCY PROPERTIES

Floriane Lignet, Vincent Calvez,
Emmanuel Grenier and Benjamin Ribba

INRIA, Project-team NUMED, Ecole Normale Supérieure de Lyon
46 allée d'Italie, 69007 Lyon Cedex 07, France

Abstract. The vascular endothelial growth factor (VEGF) is known as one of the main promoter of angiogenesis - the process of blood vessel formation. Angiogenesis has been recognized as a key stage for cancer development and metastasis. In this paper, we propose a structural model of the main molecular pathways involved in the endothelial cells response to VEGF stimuli. The model, built on qualitative information from knowledge databases, is composed of 38 ordinary differential equations with 78 parameters and focuses on the signalling driving endothelial cell proliferation, migration and resistance to apoptosis. Following a VEGF stimulus, the model predicts an increase of proliferation and migration capability, and a decrease in the apoptosis activity. Model simulations and sensitivity analysis highlight the emergence of robustness and redundancy properties of the pathway. If further calibrated and validated, this model could serve as tool to analyse and formulate new hypothesis on th e VEGF signalling cascade and its role in cancer development and treatment.

1. **Introduction.** Cancer angiogenesis is a crucial process by which endothelial cells from pre-existing blood vessels are recruited through secretion and signalling of growth factors mainly produced by tumour and stroma cells. The process leads to the formation of new blood vessels improving oxygen and nutrient supply to the tumour [21, 12]. The vascular Growth Factor (VEGF) and its receptors (VEGFRs) are often referred as key molecules of this process. The VEGF family comprises VEGF-A, VEGF-B, VEGF-C, VEGF-E, PlGF (placenta growth factor) and svVEGF(snake venom VEGF). Each of these genes can undergo alternative splicing and generate several isoforms [60]. $VEGF_{165}$ is the predominant isoform of VEGF-A and is involved in the recruitment of endothelial cells and change in vessel permeability during the process of angiogenesis [60, 19].

$VEGF_{165}$ can bind several specific tyrosine kinase receptors such as VEGFR-1 and VEGFR-2 [19]. VEGFR-2 appears to be the main receptor involved in pathological angiogenesis, and stands thus as the target of several antiangiogenic drug compounds [47]. $VEGF_{165}$ binding to the VEGFR-2 leads to the phosphorylation of the intracellular kinase domain of the receptor, which can then activate the three main molecular pathways of the endothelial cells, namely, proliferation, migration and survival [18, 13].

2010 *Mathematics Subject Classification.* Primary: 92C42, 92C45, 92E20; Secondary: 65L99.

Key words and phrases. Systems biology, networks, kinetics in biochemical problems, molecular reactions, ordinary differential equations, Vascular Endothelial Growth Factor (VEGF) signalling.

Several drugs have been developed with the aim of inhibiting the process of angiogenesis. These therapeutic compounds target the binding of VEGF to its receptors either by "capturing" the ligand before its binding or by inhibiting the phosphorylation of the receptor kinase domains which normally results from the binding [20, 17]. VEGF can be trapped by large molecules such as monoclonal antibodies (MAbs). For example, Bevacizumab is one of the famous MAbs developed to inhibit the process of angiogenesis. Receptor tyrosine kinase inhibitors (RTKis) are in general small molecules. Sunitinib and Sorafenib are two recently developed RTKis. In addition to these two classes of drugs, innovative compounds also attempt to inhibit the molecules within the signalling cascade. For instance, Enzastaurin inhibits the activation of the proteine kinase C (PKC) activation [45].

Modelling of signalling pathway is a quite recent and growing field of research also referred as "Systems Biology". Models generally consists of discrete or continuous mathematical formalisms describing the time-evolution of (part of) the molecules composing the signalling cascade. In particular, continuous models generally involve several coupled ordinary differential equations (ODEs) based on mass action kinetics and Michaelis-Menten functions.

The studies of such complex models have driven the identification of some recurrent properties. Among them, robustness, as the capacity to resist to severe perturbations, and redundancy, as alternative ways to generate an output in the face of perturbations, seem to be common emerging properties of these complex living systems [14, 7]. These two traits were also highlighted in the context of cancer development [34] and in particular for the epidermal growth factor receptor (EGFR) pathway [54, 37].

The VEGF receptor has received less attention even if the corresponding signalling cascade is partially described in the literature [47, 58, 15].

An adjacent field of research, namely "Biomathematics", is also taking advantage of systems biology models to develop multiscale models of cancer. In this approach, molecular models describing intracellular signalling pathways are coupled to cellular and/or tissue description of tumour growth and treatment. Recently, Wang and co-workers developed a multiscale model of non-small cell lung cancer growth integrating a model of the the EGFR pathway which "pilots" the behaviour of cells in a 2 dimensional lattice ([64]). Scianna and co-workers also proposed a multiscale model of vasculogenesis by coupling a cellular potts model (CPM) describing endothelial cells with a simplified partial differential equation model of VEGF-induced molecular reactions [55]. Finally, we have also proposed a multiscale model of avascular tumor growth by integrating a discrete boolean-like gene regulatory network regulating tumour cell prolifer ation, quiescence and apoptosis [52].

The objective of the present work was to develop a structural model of the signalling pathways downstream VEGFR-2 based on qualitative knowledge found in the literature and dedicated databases. The model was used as a simulation tool to explore the system and its complexity.

2. Methods.

2.1. Model building.

The model was built based on available literature knowledge and dedicated databases on gene regulatory networks. Two sources of information were mainly used to design the structure of the model. The first is Pubmed[1] from

[1] http://www.ncbi.nlm.nih.gov/sites/entrez?db=pubmed

which systematic research through the Mesh ontology was performed. The second was the Kyoto Encyclopedia for Genes and Genomes[2] (KEGG) which presents a structural map of the VEGF signalling pathway. Based on these information, our model contains three main pathways downstream the receptor VEGFR-2, namely proliferation, migration and survival. It is schematically represented in Figure 1 and relies on the following assumptions:

- $VEGF_{165}$, further simply denoted VEGF, binds to VEGFR-2 located at the surface of endothelial cells which leads to the formation of homodimers and to the auto-phosphorylation of the intracellular kinase domains [47]. This will results in an activation of the molecules at the top of three signalling cascades:
- Proliferation [15]: the phospholipase Cγ (PLCγ) is recruited and phosphorylated by the tyrosine 1175 of VEGFR-2 [13, 57]. It leads to the activation of Protein Kinase C (PKC) [49], and then the activation of the mitogen activated protein kinase (MAPK) signaling pathway through Raf, Ras, MEK (a MAPK kinase) and ERK (extracellular-signal-regulated kinase);
- Migration [39, 30]: Actin reorganization and consequent cellular migration is activated through the phosphorylation of p38 that triggers the phosphorylation of MAKPAPK (MAPK activating protein kinase) and then the phosphorylation of the heat-shock protein (Hsp27).
- Survival [25, 63]: Phosphatidylinositol-3-kinase (PI3K) is a lipid kinase whose phosphorylation through the binding to VEGFR-2 allows for the transformation of PIP2 into PIP3. PIP3 can then bind to Akt which is in turn bi-phosphorylated by the phosphoinositide-dependent Kinases (PDK). The resulting product, AktPIPP, can then phosphorylate the caspase 9 (Casp9). The phosphorylated form of Casp9P is known to prevent from apoptosis.

2.2. **Model equations.** We modelled the dynamics of reactions using mass action kinetics and described the reaction rates as proportional to the reacting molecules concentrations. For instance, in the reaction $A + B \rightleftharpoons AB$, the compounds A and B bind each other to form a stable complex AB at rate k_1. Reversely, the product AB dissociates into A and B at rate k_{-1}. The speed of the reaction is then given by:

$$v = k_1[A][B] - k_{-1}[AB]. \tag{1}$$

For some complex multistep reactions, such as phosphorylations, we used the Michaelis-Menten approximation. This allows for reducing the complexity of the system description still maintaining the main dynamical property of the reaction: For instance, $A^* + B \rightleftharpoons A^*B \to A^* + B^*$ where A^* is the so-called reaction catalyzer of the activation of B into B^* can be simplified to $A^* + B \to B^*$ given the corresponding rate equation :

$$v = \frac{V \cdot [A^*][B]}{K + [B]}, \tag{2}$$

which is the Michaelis-Menten equation. When several reactions are triggered by the same catalyzer, the rate equations can become complex as the molecules compete for the same catalyzer. In this case, the corresponding reaction rates will depend on the concentrations and kinetic properties of all the "rivals" (we invite the reader to refer to the Appendix B in [27] and Figure 3 in [3] for further technical details).

All the rate equations encompassed in the model are described in Table 1.

[2] http://www.genome.jp/kegg/pathway.html

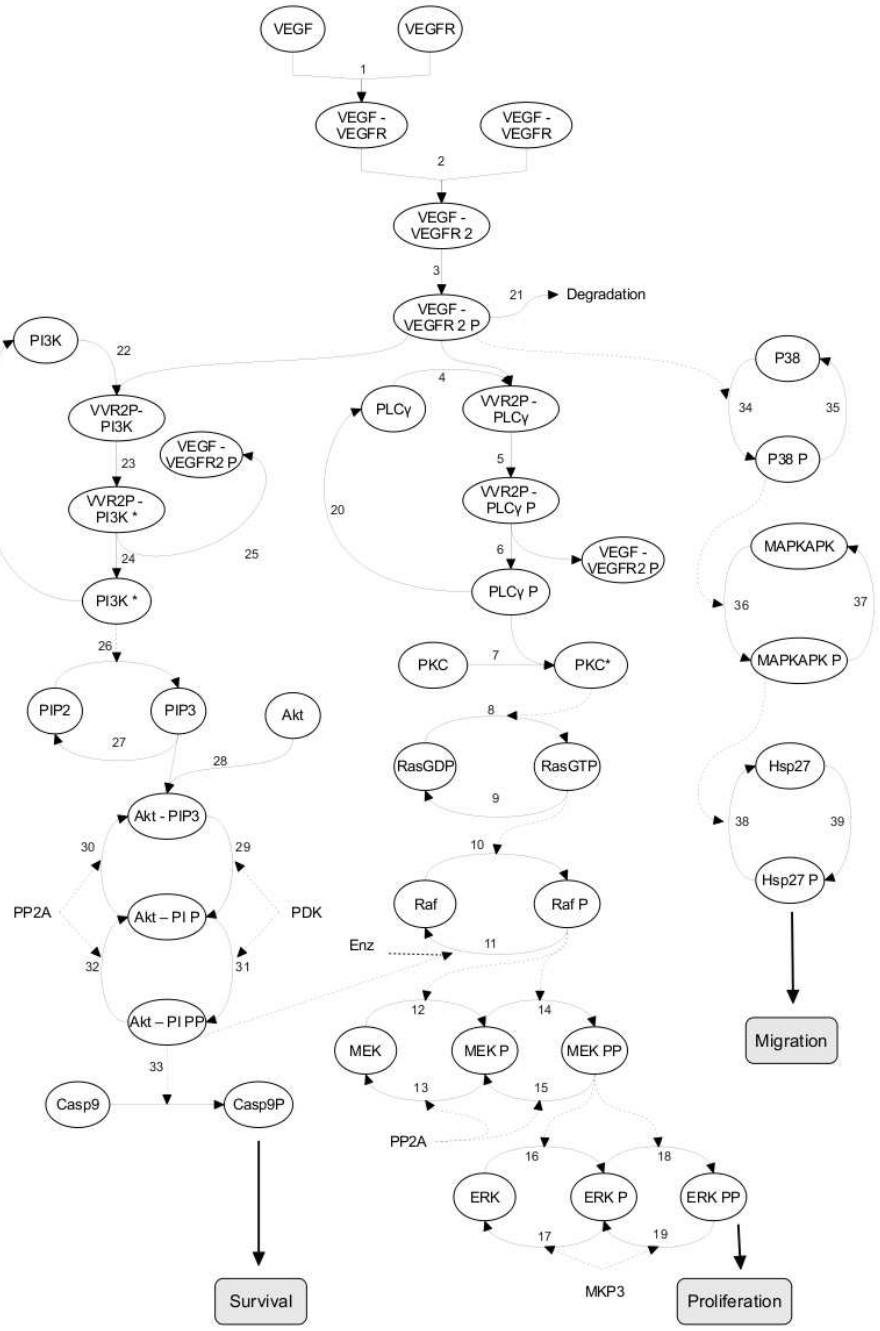

FIGURE 1. Molecular pathways of VEGFR-2 downtream signalling in endothelial cells.

In consequence, assuming the molecular concentrations continuous, and the reactions happening - on a deterministic fashion - in a homogeneous medium of a

volume large enough, we can describe the time-dynamic of each molecule of the model with an ODE:

$$\frac{dc_i}{dt} = \sum v_{prod,c_i} - \sum v_{cons,c_i}, \tag{3}$$

where v_{prod,c_i} and v_{cons,c_i} are respectively the velocities of the reactions producing and consuming the molecule c_i.

The complete set of model equations is presented in Table 2.

The model is composed by a system of 38 ordinary differential equations including 78 parameters. Solving this system provides the dynamic of all the model variables (molecules) over time. The model was implemented in Scilab[3] and function *ode*, based on the Runge-Kutta method on order 4, was used to solve our system.

2.3. **Model calibration and sensitivity analysis.** Model calibration is the process by which parameter values are identified and estimated. Experimentally, it is highly challenging to collect enough high quality data to effectively estimate parameter values. In consequence, since we did not have time series experiments of VEGF signallization to which compare our simulations, our model is calibrated on the basis of knowledge on different molecular systems, as most biological pathway models. Indeed we relied on previous published works to provide quantitative information to our model parameters. In particular, the parameters relative to the proliferation and survival pathways were taken from [27] whereas the parameters relative to the migration pathway were estimated to fit the molecules dynamics presented in [28]. All our model parameter values are presented in table 3.

To integrate these external values into our system, we fixed arbitrarily two model parameters. These parameters regulate the degradation of the phosphorylated dimer VEGF-VEGFR2 (see reaction 21 in Table 1). Obviously, these parameters are, a-priori, highly important in our model since all the three downstream pathways rely on the phosphorylated dimer. To study the influence of this parameters values on the dynamics of our system, we simulated the response of the model to a one-fold increase of VEGF stimuli for a set of twenty different values of the two parameters. We picked up these 20 values in uniformly distributed interval with length two $\log_{10}$-fold around the baseline arbitrary fixed values.

3. **Results.** Practically, to analyze the behaviour of our system, it is not feasible to represent the time-evolution of the 38 model variables. In consequence, we selected a set of three molecules to represent at best the behaviour of the three pathways. In this respect, the bi-phosphorylated extracellular-signal-regulated kinase (ERK-PP), the phosphorylated heat-shock protein 27 (Hsp27-P) and the phosphorylated Caspase 9 (Casp9-P) will always be represented in the figure results.

3.1. **Complexity of MEK/ERK loop in response to the ligand stimuli.** We first analyzed the dynamic of the modelled system in response to several intensity of VEGF stimuli. For this, the model was simulated with 5, 10 and 50 nM of VEGF stimuli (Figure 2) as the 50 nM concentration was found to correspond to the saturation concentration.

Most of the model molecules, including those of the migration and survival pathway, show a rather expected dynamic similar to the time-course profile of the VEGF signal, i.e. a quick increase to a maximum, followed by a decrease to the molecule

[3] http://www.scilab.org

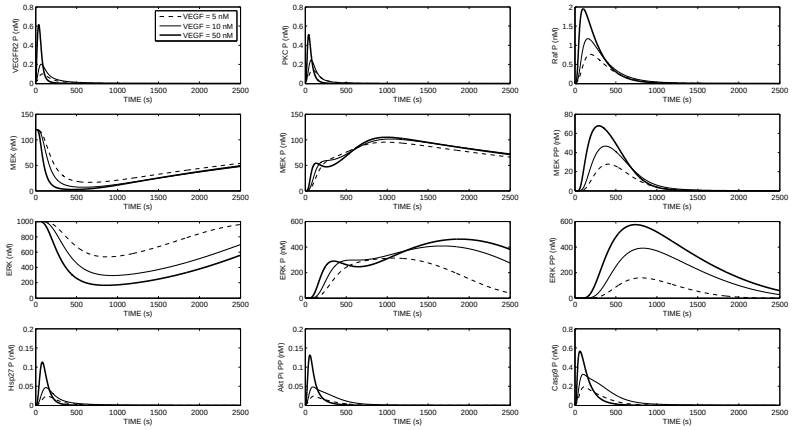

FIGURE 2. Dynamic of the main molecules in the VEGFR signalling pathway in response to different VEGF stimuli: Dashed : 5 nM, Thin : 10nM, Thick : 50nM. Included is the phosphorylated VEGFR dimer at the top left of the figure.

baseline value. However, the molecules of the proliferation pathway behave quite differently, in particular the MEK and ERK forms. First of all, MEK, ERK, MEK-PP and ERK-PP react with an important delay. Then, for MEK-P and ERK-P a local maximum appears for the highest VEGF concentration. However, this seems to have no consequence on the downstream molecules MEK-PP and ERK-PP. These results highlight the complex dynamic of the MEK/ERK loop characterized by highly different values of reaction rates so that reactions can be slowed down at a certain stage of the pathway and be further accelerated at a successive stage.

To analyze in more detail the effect of the increase of VEGF, we represented in Figure 3 the variation of maximum value reached for each molecule and the variation of the time at which this maximum is reached when the concentration of VEGF increases by one fold, from 5 to 10 nM (note: for molecules whose amount is reduced by the normal activation of the pathway, by consumption or phosphorylation, we consider the minimum value reached and the time at which it is reached). For most of the network molecules, such a ligand concentration increase leads to a faster reaction (on average -10% of time needed to reach the maximum value) and an higher maximum value (increase between 50 and 100%), as it is expected. But for the MEK/ERK, activation seems to be delayed; in particular for ERK-P, whose maximum appears significantly delayed when the VEGF stimuli increases. ERK-PP signal is also increased by 146% while slightly delayed in time.

3.2. **System robustness and emergence of redundancy.** When analyzing the sensitivity of our system to a change in the two constant rates of the phosphorylated dimer VEGF-VEGFR2 degradation, by considering the impact of these parameters changes on the response of the system to a two fold increase of VEGF stimulation. The dynamics observed for each molecule remain comparable to the dynamics presented in fig 2. We observed that only the ERK forms (at the bottom of the pathway) were sensitive to the changes of the constant rates values (see Figure 4

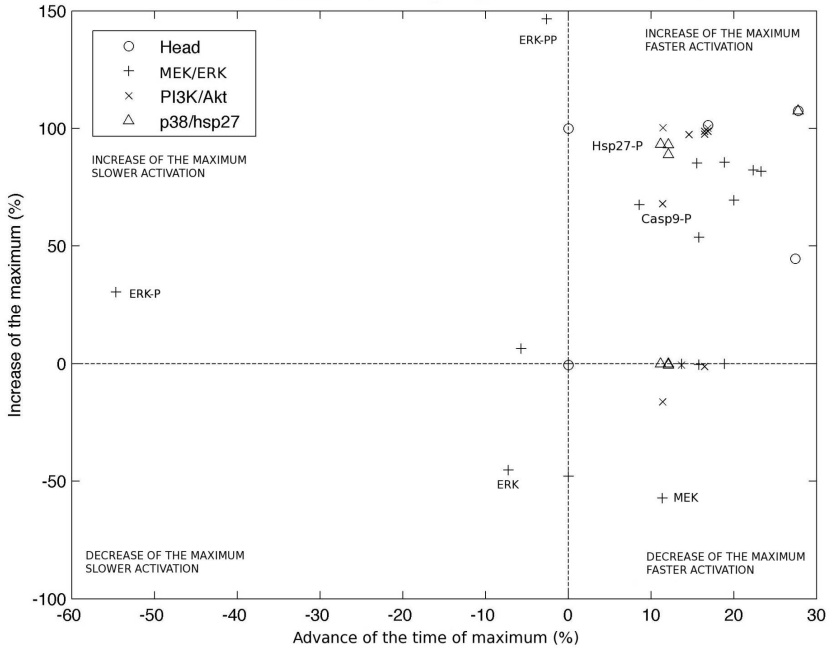

FIGURE 3. Variation of the value of the maximum (resp. the minimum for consumed molecules) versus the variation of time to reach the maximum (resp. the minimum), in %, with respect to a stimulus of 5nM of VEGF, when VEGF stimulus increases by one-fold, from 5 to 10 nM. The molecules are represented depending on the branch they belong to. Circles represent the molecules of the head of the signalling pathway, meaning VEGF, VEGFR and all the compounds formed by their association. Crosses are the molecules of the proliferation branch, leading to the phosphorylation of MEK and ERK. Xs are the molecules of the survival branch, that activates PI3K and Casp9. Triangles are the molecules of the migration branch, whose main actors are Hsp27 and p38.

and Figure 5). Interestingly, the changes do not affect the qualitative effect of VEGF stimuli increases which still leads to a delay in the response of ERK-P, a lower maximum for ERK, and an increase of the maximal amount of ERK-PP. No other molecules seem to be affected by these changes. In conclusion, the system is globally robust to the change in the values of these two important constant rates.

Finally, we also simulated the blockade of particular molecules within the pathway by reducing the speed of their corresponding activating reactions. As before, we evaluated the variation of the amplitude of the maximum concentration reached by the different molecules as well as the time at which this maximum is reached. We decided to focus on the consequences of a blockade of PKC phosphorylation (reaction number 7 on fig. 1, in the proliferation pathway) and Akt binding to PIP3 (reaction number 28 on fig. 1, in the survival pathway). These blockade were

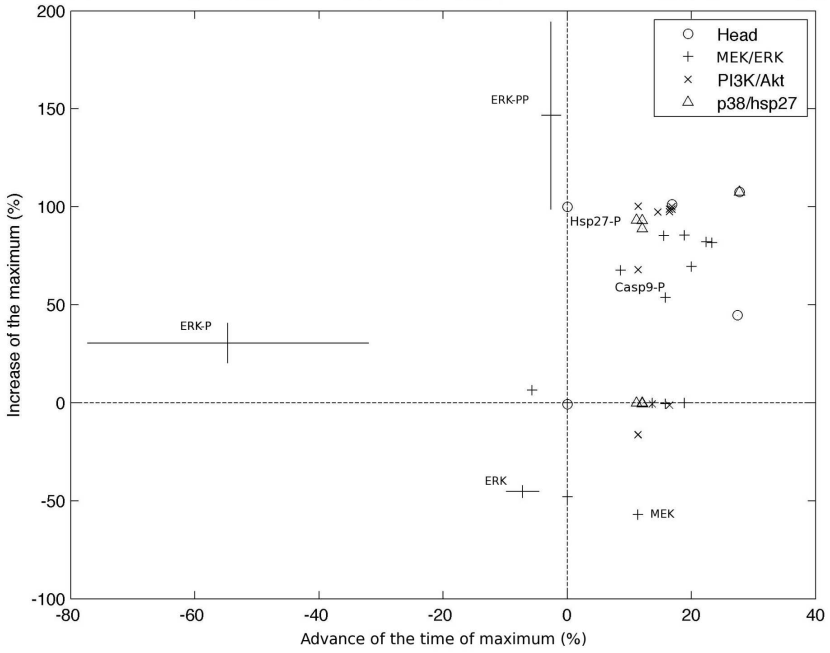

FIGURE 4. Influence of a modification in the value of the constant rate k21, involved in the phosphorylated dimer VEGF-VEGFR2 degradation, on the system measured as a change in the value of the maximum (resp. the minimum for consumed molecules) reached (y-axis) and in the time at which this maximum (resp. minimum) is reached (x-axis). The bars represent the range of the variation when the value of k21 is increased or decreased ten fold.

achieved by modifying the reaction parameters to values that leads to a reduction by half of the maximal amount of molecules normally produced by these reactions (respectively PKC-P and Akt-PIP3).

The blockade of PKC phosphorylation leads to a decrease of the maximum amount of ERK-PP secreted (more than 25% decrease compared to the unblocked situation), to which corresponds an accumulation of the non phosphorylated form ERK (see Figure 6). An interesting point is the simultaneous slight increase of Casp9 related to a decrease of its phosphorylation into Casp9-P. ERK-PP being related to the cellular proliferation, and Casp9 to the survival pathway (Casp9-P is the inactivated form, i.e. the phosphorylation of Casp9 triggers a resistance to apoptosis and thus survival), this results means that inhibiting proliferation by targeting PKC confer to the cell a higher sensitivity to apoptosis. This demonstrates the redundancy of the system towards an inhibition of the proliferation pathway.

Reversely, we also observed a slight reduction of the proliferation activity, in terms of time at which ERK and ERK-PP reach maximum, when inhibiting the binding of Akt to PIP3. Even if this reduction is not significant, it highlights the link between the proliferation and apoptotic pathways. The blockade Akt binding

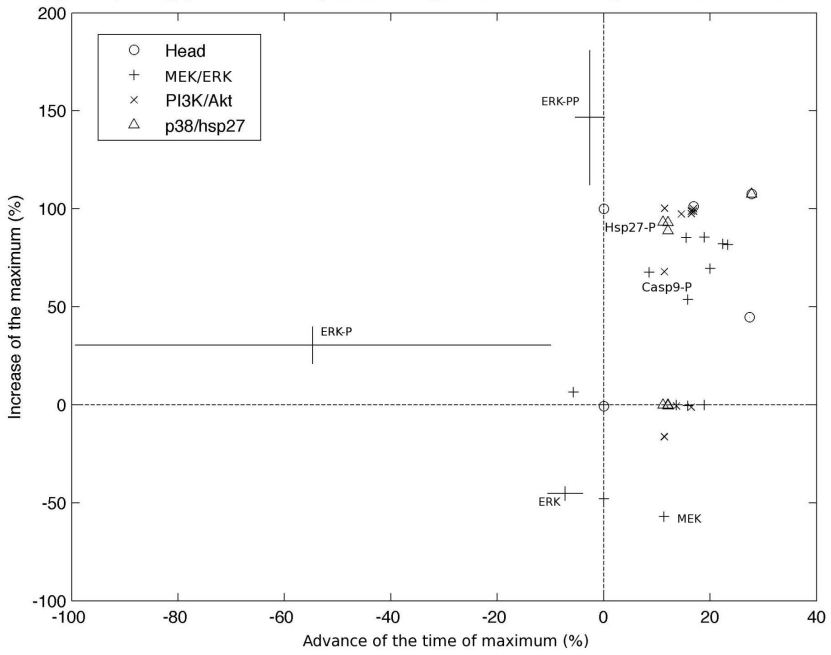

FIGURE 5. Influence of a modification in the value of the constant rate km21, involved in the phosphorylated dimer VEGF-VEGFR2 degradation, on the system measured as a change in the value of the maximum (resp. the minimum for consumed molecules) reached (y-axis) and in the time at which this maximum (resp. minimum) is reached (x-axis). The bars represent the range of the variation when the value of k21 is increased or decreased ten fold.

mainly leads to an accumulation of Casp9 (see Figure 7) linked to a reduction of the phosphorylated, apoptotic resistance related form Casp9.

4. **Discussion.** Based on literature information from Pubmed and from the Kyoto Encyclopedia for Genes and Genomes (KEGG), we developed a model of the VEGFR-2 intracellular signalling pathway. This model mainly focuses on the proliferation, migration and survival pathways of the endothelial cells composing blood vessels. With parameter values taken from existing publications, the model was used as a simulation tool to analyse the complexity of the underlying system.

Some remarks need to be formulated regarding the structure of our model. First, we limited our analysis to the pathways triggering proliferation, migration and survival of the endothelial cells, whereas VEGFR-2 is known to drive also variations of the vascular permeability. We omitted this feature since we found contradictory information on how permeability was driven by the VEGFR-2 signalling network. It also appears that change in the vascular permeability may significantly depends on the shape and adhesion properties of the cells composing the vessels [15, 47].

We also chose to not consider the genetic mechanisms triggered by the studied signalling pathways. In particular, transition from ERK-PP, Hsp27-P or Casp9-P

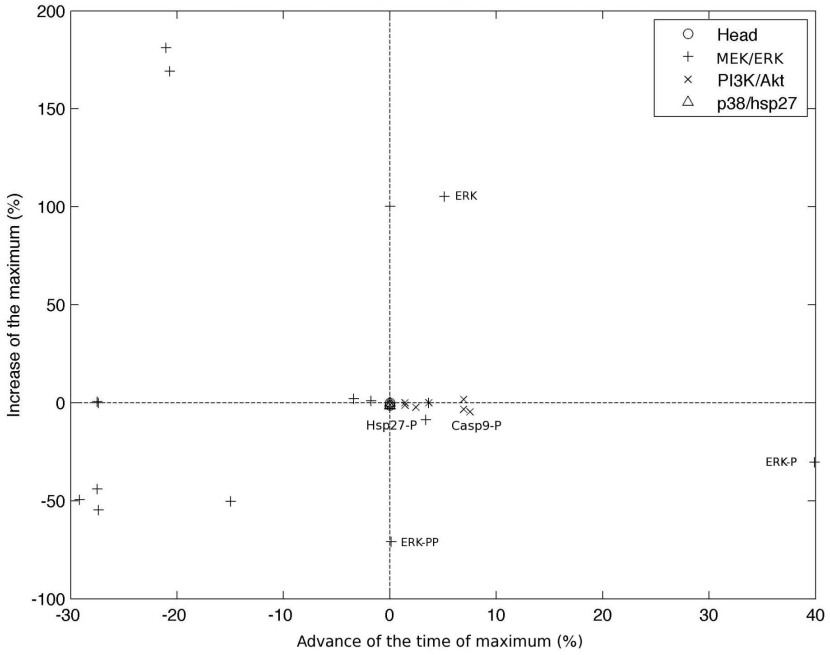

FIGURE 6. Influence of a blocking in PKC phosphorylation, on the system measured as a change in the value of the maximum (resp. the minimum for consumed molecules) reached (y-axis) and in the time at which this maximum (resp. minimum) is reached (x-axis).

involve complex processes that go from DNA transcription to protein synthesis. We decided to limit our description at the cytoplasmic level (in opposition to the nucleic level). We also described the receptor dynamic with simple laws of action mass kinetics in order to have a consistent level of description in the whole model whereas complex models of VEGFR-2 dimerization have already been proposed (see for instance [2]). Finally, we did not consider the variation of receptor density at the surface of endothelial cells that can be observed during angiogenic processes, as VEGFR-2 concentration is up-regulated by hypoxia [47] and by cell density [44].

It is also worthwhile to mention that special standards and methods [3, 46, 10] as well as tools [35, 4], not used in the present work, have been proposed for homogenizing the development and encoding of this type of systems biology models.

Still, our model simulations revealed two important features of complex living systems. We first highlighted the complexity and difference in the dynamics of the proliferation, migration and survival pathways downstream the VEGF receptor. The proliferation pathway appeared to be the most sensitive, with peculiar response, to an increase of the VEGF input. However, its increase was delayed in time with respect to the migration and survival pathways. In addition to that, robustness emerged when perturbing the system with a change in the upstream parameters involved in the phosphorylated dimer VEGF-VEGFR2 degradation, and redundancy occurred between the proliferation and the survival pathways. This

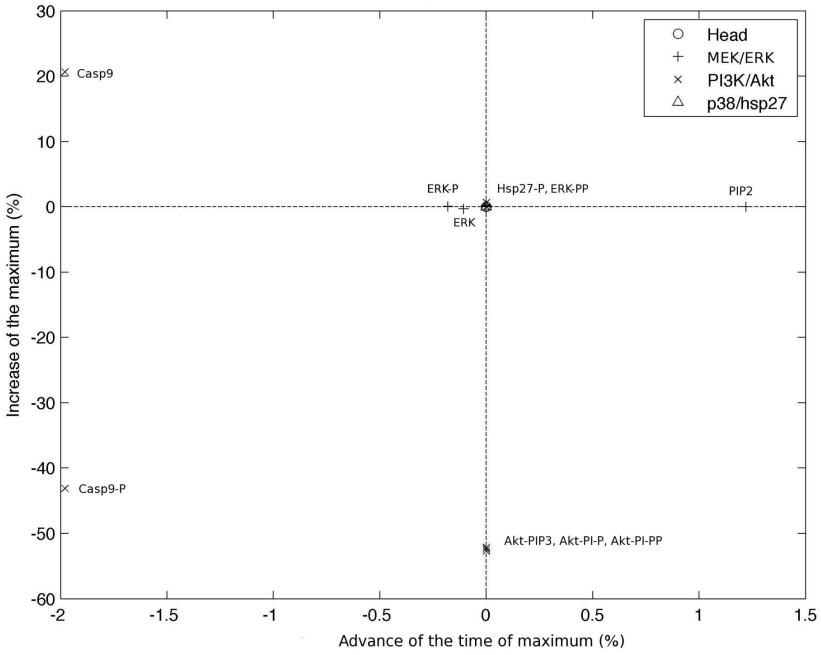

FIGURE 7. Influence of inhibiting the binding of Akt to PIP3 which leads to an accumulation of Casp9, on the system measured as a change in the value of the maximum (resp. the minimum for consumed molecules) reached (y-axis) and in the time at which this maximum (resp. minimum) is reached (x-axis).

model, being a qualitative tool, appears to be potentially interesting to analyze and formulate new hypothesis on the VEGF signalling cascade.

As most of biomathematicians, working in the field of cancer modelling, attempt to build multiscale model with integrated molecular pathways, our model could serve as the molecular piece of the puzzle to reach an holistic and integrative framework of tumour growth and treatment.

Acknowledgments. FL and BR wish to acknowledge the team "EMR UCBL/HCL 3738, Faculté de Médecine Lyon-Sud, Université Claude Bernard Lyon 1, Lyon, France" and its head Prof. Gilles Freyer for having hosting them during the very early start of this work.

Reaction	Rate equation
v_1	$k_1\,[VEGF]\,[VEGFR] - km_1\,[VEGF.VEGFR]$
v_2	$k_2\,[VEGF.VEGFR]^2 - km_2\,[VEGF.VEGFR2]$
v_3	$k_3\,[VEGF.VEGFR2] - km_3\,[VEGF.VEGFR2P]$
v_4	$k_4\,[VEGF.VEGFR2P]\,[PLC\gamma] - km_4\,[VEGF.VEGFR2P.PLC_\gamma s]$
v_5	$k_5\,[VEGF.VEGFR2P.PLC_\gamma] - km_5[VEGF.VEGFR2P.PLC_\gamma P]$
v_6	$k_6\,[VEGF.VEGFR2P.PLC_\gamma P] - km_6\,[PLC\gamma P]\,[VEGF.VEGFR2P]$
v_7	$k_7\,[PLC\gamma P][PKC] - km_7\,[PKC*]$
v_8	$V_8\,[PKC*]\,[RasGDP]/(K_8 + [RasGDP])$
v_9	$V_9\,[RasGTP]/(K_9 + [RasGTP])$
v_{10}	$V_{10}\,[RasGTP][Raf]/(K_{10} + [Raf])$
v_{11}	$V_{11}\,(AktPIPP + Enz)\,[RafP]/(K_{11} + [RafP])$
v_{12}	$V_{12}\,[RafP][MEK]/(K_{12}\,(1 + \frac{[MEKP]}{K_{14}}) + [MEK])$
v_{13}	$V_{13}\,[PP2A][MEKP]/(K_{13}\,(1 + \frac{[MEKPP]}{K_{15}} + \frac{[AktPIP]}{K_{30}} + \frac{[AktPIPP]}{K_{32}}) + [MEKP])$
v_{14}	$V_{14}\,[RafP][MEKP]/(K_{14}\,(1 + \frac{[MEK]}{K_{12}}) + [MEKP])$
v_{15}	$V_{15}\,[PP2A][MEKPP]/(K_{15}\,(1 + \frac{[MEKP]}{K_{13}} + \frac{[AktPIP]}{K_{30}} + \frac{[AktPIPP]}{K_{32}}) + [MEKPP])$
v_{16}	$V_{16}\,[MEKPP]\,[ERK]/(K_{16}\,(1 + \frac{[ERKP]}{K_{18}}) + [ERK])$
v_{17}	$V_{17}\,[MKP3]\,[ERKP]/(K_{17}\,(1 + \frac{[ERKPP]}{K_{19}}) + [ERKP])$
v_{18}	$V_{18}\,[MEKPP]\,[ERKvP]/(K_{18}\,(1 + \frac{[ERK]}{K_{16}}) + [ERKP])$
v_{19}	$V_{19}\,[MKP3]\,[ERKPP]/(K_{19}\,(1 + \frac{[ERKP]}{K_{17}}) + [ERKPP])$
v_{20}	$V_{20}\,[PLC\gamma P]/(K_{20} + [PLC\gamma P])$
v_{21}	$V_{21}\,[VEGF.VEGFR2P]/(K_{21} + [VEGF.VEGFR2P])$
v_{22}	$k_{22}\,[PI3K]\,[VEGF.VEGFR2P] - km_{22}\,[VEGF.VEGFR2P.PI3K]$
v_{23}	$k_{23}\,[VEGF.VEGFR2P.PI3K] - km_{23}\,[VEGF.VEGFR2P.PI3K*]$
v_{24}	$k_{24}\,[VEGF.VEGFR2P.PI3K*] - km_{24}\,[VEGF.VEGFR2P]\,[PI3K*]$
v_{25}	$V_{25}\,[PI3K*]/(K_{25} + [PI3K*])$
v_{26}	$V_{26}\,[PI3K*]\,[PIP2]/(K_{26} + [PIP2])$
v_{27}	$V_{27}\,[PIP3]/(K_{27} + [PIP3])$
v_{28}	$k_{28}\,[PIP3]\,[Akt] - km_{28}[Akt.PIP3]$
v_{29}	$V_{29}\,[PDK]\,[Akt.PIP3]/(K_{29}\,(1 + \frac{[AktPIP]}{K_{31}}) + [Akt.PIP3])$
v_{30}	$V_{30}\,[PP2A]\,[AktPIP]/(K_{30}\,(1 + \frac{[MEKP]}{K_{13}} + \frac{[MEKPP]}{K_{15}} + \frac{[AktPIPP]}{K_{32}}) + [AktPIP])$
v_{31}	$V_{31}\,[PDK]\,[AktPIP]/(K_{31}\,(1 + \frac{[Akt.PIP3]}{K_{29}}) + [AktPIP])$
v_{32}	$V_{32}\,[PP2A]\,[AktPIPP]/(K_{32}\,(1 + \frac{[MEKP]}{K_{13}} + \frac{[MEKPP]}{K_{15}} + \frac{[AktPIP]}{K_{30}}) + [AktPIPP])$
v_{33}	$k_{33}\,[AktPIPP]\,[Casp9] - km_{33}\,[Casp9P]$
v_{34}	$V_{34}\,[VEGF.VEGFR2P][P38]/(K_{34} + [P38])$
v_{35}	$V_{35}\,[P38P]/(K_{35} + [P38P])$
v_{36}	$V_{36}\,[P38P][MAPKAPK]/(K_{36} + [MAPKAPK])$
v_{37}	$V_{37}\,[MAPKAPK.P]/(K_{37} + [MAPKAPK.P])$
v_{38}	$V_{38}\,[MAPKAPK.P][Hsp27]/(K_{38} + [Hsp27])$
v_{39}	$V_{39}\,[Hsp27P]/(K_{39} + [Hsp27P])$

TABLE 1. Reactions and rate equations of the model.

Molecule	Differential equation
$VEGF$	$-v_1$
$VEGFR$	$-v_1$
$VEGF.VEGFR$	$v_1 - 2 * v_2$
$VEGF.VEGFR2$	$v_2 - v_3$
$VEGF.VEGFR2P$	$v_3 - v_4 + v_6 - v_{21} - v_{22} + v_{24}$
PLC_γ	$-v_4 + v_{20}$
$VEGF.VEGFR2P.PLC_\gamma$	$v_4 - v_5$
$VEGF.VEGFR2P.PLC_\gamma P$	$v_5 - v_6$
$PLC_\gamma P$	$v_6 - v_7 - v_{20}$
PKC	$-v_7$
$PKC*$	v_7
$RasGDP$	$-v_8 + v_9$
$RasGTP$	$v_8 - v_9$
Raf	$-v_{10} + v_{11}$
$RafP$	$v_{10} - v_{11}$
MEK	$-v_{12} + v_{13}$
$MEKP$	$v_{12} - v_{13} - v_{14} + v_{15}$
$MEKPP$	$v_{14} - v_{15}$
ERK	$-v_{16} + v_{17}$
$ERKP$	$v_{16} - v_{17} - v_{18} + v_{19}$
$ERKPP$	$v_{18} - v_{19}$
$PI3K$	$-v_{22} + v_{25}$
$VEGF.VEGFR2P.PI3K$	$v_{22} - v_{23}$
$VEGF.VEGFR2P.PI3K*$	$v_{23} - v_{24}$
$PI3K*$	$v_{24} - v_{25}$
$PIP2$	$-v_{26} + v_{27}$
$PIP3$	$v_{26} - v_{27} - v_{28}$
Akt	$-v_{28}$
$Akt.PIP3$	$v_{28} - v_{29} + v_{30}$
$Akt.PI.P$	$v_{29} - v_{30} - v_{31} + v_{32}$
$Akt.PI.PP$	$v_{31} - v_{32} - v_{33}$
$Casp9$	$-v_{33}$
$Casp9P$	v_{33}
$P38$	$-v_{34} + v_{35}$
$P38P$	$v_{34} - v_{35}$
$MAPKAPK$	$-v_{36} + v_{37}$
$MAPKAPKP$	$v_{36} - v_{37}$
$Hsp27$	$-v_{38} + v_{39}$
$HSP27P$	$v_{38} - v_{39}$

TABLE 2. List of all molecules and corresponding equations

Parameter	Value	Source	Parameter	Value	Source
k_1	0.0012	[27]	km_1	0.00076	[27]
k_2	0.01	[27]	km_2	1	[27]
k_3	1	[27]	km_3	0.01	[27]
k_4	0.06	[64]	km_4	0.2	[64]
k_5	1	[64]	km_5	0.05	[64]
k_6	0.3	[64]	km_6	0.006	[64]
k_7	0.214	[64]	km_7	5.35	[64]
V_8	0.222	[27]	K_8	0.181	[27]
V_9	0.289	[27]	K_9	0.0571	[27]
V_{10}	1.53	[27]	K_{10}	11.7	[27]
V_{11}	0.00673	[27]	K_{11}	8.07	[27]
V_{12}	3.5	[27]	K_{12}	317	[27]
V_{13}	0.058	[27]	K_{13}	2200	[27]
V_{14}	2.9	[27]	K_{14}	317	[27]
V_{15}	0.058	[27]	K_{15}	60	[27]
V_{16}	9.5	[27]	K_{16}	146000	[27]
V_{17}	0.3	[27]	K_{17}	160	[27]
V_{18}	16	[27]	K_{18}	146000	[27]
V_{19}	0.27	[27]	K_{19}	60	[27]
V_{20}	1	[64]	K_{20}	100	[64]
V_{21}	6	Est	K_{21}	50	Est.
k_{22}	0.1	[27]	km_{22}	2	[27]
k_{23}	9.85	[27]	km_{23}	0.0985	[27]
k_{24}	45.8	[27]	km_{24}	0.047	[27]
V_{25}	2620	[27]	K_{25}	3680	[27]
V_{26}	16.9	[27]	K_{26}	39.1	[27]
V_{27}	17000	[27]	K_{27}	9.02	[27]
k_{28}	507	[27]	km_{28}	234	[27]
V_{29}	20000	[27]	K_{29}	80000	[27]
V_{30}	0.107	[27]	K_{30}	4.35	[27]
V_{31}	20000	[27]	K_{31}	80000	[27]
V_{32}	0.211	[27]	K_{32}	12	[27]
k_{33}	1	Est.	km_{33}	0.1	Est.
V_{34}	0.1	Est.	K_{34}	20	Est.
V_{35}	1	Est.	K_{35}	50	Est.
V_{36}	0.1	Est.	K_{36}	5	Est.
V_{37}	1	Est.	K_{37}	0.01	Est.
V_{38}	10	Est.	K_{38}	10	Est.
V_{39}	1	Est.	K_{39}	10	Est.
PDK	1	[27]	$PP2A$	11.4	[27]
$MKP3$	2.4	[27]	Enz	7	[27]

TABLE 3. Molecular model parameters. Michaelis-Menten constants ($K_8 \to K_{21}$, K_{25}, K_{26}, K_{27}, $K_{29} \to K_{32}$, $K_{34} \to K_{39}$) are given in nM. $V_8 \to V_{21}$, V_{25}, V_{26}, V_{27}, $V_{29} \to V_{32}$, $V_{34} \to V_{39}$ are expressed in $nM.s^{-1}$. First- and second-order rate constants are given in s^{-1} and $nM^{-1}.s^{-1}$ respectively. The bottom of the table presents the constant concentrations of the enzymes, in nM.

REFERENCES

[1] T. Alarcón, H. M. Byrne and P. K. Maini, *A multiple scale model for tumor growth*, Multiscale Modeling and Simulation, **3** (2005), 440–475.

[2] T. Alarcón and K. M. Page, *Mathematical models of the VEGF receptor and its role in cancer therapy*, Journal of The Royal Society Interface, **4** (2007), 283–304.

[3] B. B. Aldridge, J. M. Burke, D. A. Lauffenburger and P. K. Sorger, *Physicochemical modelling of cell signalling pathways*, Nature Cell Biology, **8** (2006), 1195–1203.

[4] R. Alves, F. Antunes and A. Salvador, *Tools for kinetic modeling of biochemical networks*, Nature Biotechnology, **24** (2006), 667–672.

[5] A. R. A. Anderson and M. A. J. Chaplain, *Continuous and discrete mathematical models of tumor-induced angiogenesis*, Bulletin of Mathematical Biology, **60** (1998), 857–899.

[6] R. P. Araujo and D. L. S McElwain, *A history of the study of solid tumour growth: the contribution of mathematical modelling*, Bulletin of Mathematical Biology, **66** (2004) 1039–1091.

[7] U. S. Bhalla, R. Iyengar and others, *Emergent properties of networks of biological signaling pathways*, Science, **283** (1999), 381–387.

[8] K. Bartha and H. Rieger, *Vascular network remodeling via vessel cooption, regression and growth in tumors*, Journal of Theoretical Biology, **241** (2006), 903–918.

[9] F. Billy, B. Ribba, O. Saut, H. Morre-Trouilhet, T. Colin, D. Bresch, J. P. Boissel, E. Grenier and J. P. Flandrois, *A pharmacologically based multiscale mathematical model of angiogenesis and its use in investigating the efficacy of a new cancer treatment strategy*, Journal of Theoretical Biology, **260** (2009), 545–562.

[10] J. P. Boissel, B. Ribba, E. Grenier, G. Chapuisat and M-A. Dronne, *Modelling methodology in physiopathology*, Progress in Biophysics and Molecular Biology, **97** (2008), 28–39.

[11] H. M. Byrne and M. A. J. Chaplain, *Growth of nonnecrotic tumors in the presence and absence of inhibitors*, Mathematical Biosciences, **130** (1995), 151–181.

[12] P. Carmeliet and R. K. Jain, *Angiogenesis in cancer and other diseases*, Nature, **407** (2000), 249–257.

[13] S. Cebe-Suarez, A. Zehnder-Fjällman and K. Ballmer-Hofer, *The role of VEGF receptors in angiogenesis; complex partnerships*, Cellular and Molecular Life Sciences, **63** (2006), 601–615.

[14] A. Citri and Y. Yarden, *EGF–ERBB signalling: Towards the systems level*, Nature Reviews Molecular Cell Biology, **7** (2006), 505–516.

[15] M. J. Cross, J. Dixelius, T. Matsumoto and L. Claesson-Welsh, *VEGF-receptor signal transduction*, Trends in Biochemical Sciences, **28** (2003), 488–494.

[16] A. Emde, C. R. Pradeep, D. A. Ferraro, N. Ben-Chetrit, M. Sela, B. Ribba, Z. Kam and Y. Yarden, *Combining epitope-distinct antibodies to HER2: cooperative inhibitory effects on invasive growth*, Oncogene, **30** (2010), 1631–1642.

[17] S. Faivre, G. Demetri, W. Sargent and E. Raymond, *Molecular basis for sunitinib efficacy and future clinical development*, Nature Reviews Drug Discovery, **6** (2007), 734–745.

[18] N. Ferrara, *VEGF and the quest for tumour angiogenesis factors*, Nature Reviews Cancer, **2** (2002), 795–803.

[19] N. Ferrara, *Vascular endothelial growth factor: basic science and clinical progress*, Endocrine Reviews, **25** (2004), 581–611.

[20] N. Ferrara, K. J. Hillan and W. Novotny, *Bevacizumab (Avastin), a humanized anti-VEGF monoclonal antibody for cancer therapy*, Biochemical and Biophysical Research Communications, **333** (2005), 326–335.

[21] J. Folkman, *Tumor angiogenesis factor*, Cancer Research, **34** (1974), 2109.

[22] J. Folkman, *New perspectives in clinical oncology from angiogenesis research*, European Journal of Cancer (Oxford, England: 1990), **32** (1996), 2534.

[23] F. M. Gabhann and A. S. Popel, *Systems biology of vascular endothelial growth factors*, Microcirculation, **15** (2008), 715–738.

[24] G. Gasparini, R. Longo, M. Fanelli and B. A. Teicher, *Combination of antiangiogenic therapy with other anticancer therapies: results, challenges, and open questions*, Journal of Clinical Oncology, **23** (2005), 1295–1311.

[25] H. P. Gerber, A. McMurtrey, J. Kowalski, M. Yan, B. A. Keyt, V. Dixit and N. Ferrara, *Vascular endothelial growth factor regulates endothelial cell survival through the phosphatidylinositol 3-kinase/Akt signal transduction pathway*, Journal of Biological Chemistry, **273** (1998), 30336–30343.

[26] F. Graner and J. A. Glazier, *Simulation of biological cell sorting using a two-dimensional extended Potts model*, Physical Review Letters, **69** (1992), 2013–2016.

[27] M. Hatakeyama, S. Kimura, T. Naka, T. Kawasaki, N. Yumoto, M. Ichikawa, J. H. Kim, K. Saito, M. Saeki, M. Shirouzu, S. Yokoyama and A. Konagaya, *A computational model on the modulation of mitogen-activated protein kinase (MAPK) and Akt pathways in heregulin-induced ErbB signalling*, Biochemical Journal, **373** (2003), 451–463.

[28] B. S. Hendriks, F. Hua and J. R. Chabot, *Analysis of mechanistic pathway models in drug discovery: p38 pathway*, Biotechnology Progress, **24** (2008), 96–109.

[29] C. Y. Huang and J. E. Ferrell, *Ultrasensitivity in the mitogen-activated protein kinase cascade*, Proceedings of the National Academy of Sciences, **93** (1996), 10078–10083.

[30] C. Huang, K. Jacobson and M. D. Schaller, *MAP kinases and cell migration*, Journal of Cell Science, **117** (2004), 4619–4628.

[31] R. K Jain, *Normalizing tumor vasculature with anti-angiogenic therapy: A new paradigm for combination therapy*, Nature Medicine, **7** (2001), 987–989.

[32] R. K Jain, *Normalization of tumor vasculature: An emerging concept in antiangiogenic therapy*, Science, **307** (2005), 58–62.

[33] H. Kitano, *Computational systems biology*, Nature, **420** (2002), 206–210.

[34] H. Kitano, *Cancer robustness: tumour tactics*, Nature, **426** (2003), 125–125.

[35] H. Kitano, A. Funahashi, Y. Matsuoka and K. Oda, *Using process diagrams for the graphical representation of biological networks*, Nature Biotechnology, **23** (2005), 961–966.

[36] M. Kohandel, M. Kardar, M. Milosevic and S. Sivaloganathan, *Dynamics of tumor growth and combination of anti-angiogenic and cytotoxic therapies*, Physics in Medicine and Biology, **52** (2007), 3665–3677.

[37] B. N. Kholodenko, O. V. Demin, G. Moehren and J. B. Hoek, *Quantification of short term signaling by the epidermal growth factor receptor*, Journal of Biological Chemistry, **274** (1999), 30169–30181.

[38] B. N. Kholodenko, *Negative feedback and ultrasensitivity can bring about oscillations in the mitogen-activated protein kinase cascades*, European Journal of Biochemistry, **267** (2001), 1583–1588.

[39] L. Lamalice, F. Le Boeuf and J. Huot, *Endothelial cell migration during angiogenesis*, Circulation Research, **100** (2007), 782–794.

[40] D. S. Lee, H. Rieger and K. Bartha, *Flow correlated percolation during vascular remodeling in growing tumors*, Physical Review Letters, **96** (2006), 58104.

[41] J. Ma and D. J. Waxman, *Combination of antiangiogenesis with chemotherapy for more effective cancer treatment*, Molecular Cancer Therapeutics, **7** (2008), 3670–3684.

[42] N. V. Mantzaris, S. Webb and H. G. Othmer, *Mathematical modeling of tumor-induced angiogenesis*, Journal of Mathematical Biology, **49** (2004), 111-187.

[43] D. B. Mendel, A. D. Laird, X. Xin, S. G. Louie, J. G. Christensen, G. Li, R. E. Schreck, T. J. Abrams, T. J. Ngai, L. B. Lee and others, *In vivo antitumor activity of SU11248, a novel tyrosine kinase inhibitor targeting vascular endothelial growth factor and platelet-derived growth factor receptors*, Clinical Cancer Research, **9** (2003), 327–337.

[44] L. Napione, S. Pavan, A. Veglio, A. Picco, G. Boffetta, A. Celani, G. Seano, L. Primo, A. Gamba and F. Bussolino, *Unraveling the influence of endothelial cell density on VEGF-A signaling*, Blood (2012), 5599–5607.

[45] N. Normanno, A. Morabito, A. De Luca, M. C. Piccirillo, M. Gallo, M. R. Maiello and F. Perrone, *Target-based therapies in breast cancer: current status and future perspectives*, Endocrine-related cancer, **16** (2009), 675–702.

[46] N. Le Novere, A. Finney, M. Hucka, U. S. Bhalla, F. Campagne, J. Collado-Vides, E. J. Crampin, M. Halstead, E. Klipp, P. Mendes and others, *Minimum information requested in the annotation of biochemical models (MIRIAM)*, Nature Biotechnology, **23** (2005), 1509–1515.

[47] A. K. Olsson, A. Dimberg, J. Kreuger and L. Claesson-Welsh, *VEGF receptor signalling-in control of vascular function*, Nat. Rev. Mol. Cell. Biol., **7** (2006), 357–371.

[48] T. M Pawlik and K. Keyomarsi, *Role of cell cycle in mediating sensitivity to radiotherapy*, International Journal of Radiation Oncology, Biology, Physics, **59** (2004), 928–942.

[49] N. Rahimi, *Vascular endothelial growth factor receptors: molecular mechanisms of activation and therapeutic potentials*, Experimental Eye Research, **83** (2006), 1005–1016.

[50] B. Ribba, O. Saut, T. Colin, D. Bresch, E. Grenier and J. P. Boissel, *A multiscale mathematical model of avascular tumor growth to investigate the therapeutic benefit of anti-invasive agents*, Journal of Theoretical Biology, **243** (2006), 532–541.

[51] B. Ribba, B. You, M. Tod, P. Girard, B. Tranchand, V. Trillet-Lenoir and G. Freyer, *Chemotherapy may be delivered based on an integrated view of tumour dynamics*, IET Systems Biology, **3** (2009), 180–190.

[52] B. Ribba, T. Colin and S. Schnell, *A multiscale mathematical model of cancer, and its use in analyzing irradiation therapies*, Theoretical Biology and Medical Modelling, **3** (2006).

[53] S. Sanga, J. P. Sinek, H. B. Frieboes, M. Ferrari, J. P. Fruehauf and V. Cristini, *Mathematical modeling of cancer progression and response to chemotherapy*, Expert review of anticancer therapy, **6** (2006), 1361–1376.

[54] B. Schoeberl, C. Eichler-Jonsson, E. D. Gilles and G. Muller, *Computational modeling of the dynamics of the MAP kinase cascade activated by surface and internalized EGF receptors*, Nature biotechnology, **20** (2002), 370–375.

[55] M. Scianna, L. Munaron and L. Preziosi, *A multiscale hybrid approach for vasculogenesis and related potential blocking therapies*, Progress in Biophysics and Molecular Biology, **106** (2011), 450–462.

[56] S. Senan and E. F. Smit, *Design of clinical trials of radiation combined with antiangiogenic therapy*, The Oncologist, **12** (2007), 465–477.

[57] M. Shibuya, *Differential roles of vascular endothelial growth factor receptor-1 and receptor-2 in angiogenesis.*, Journal of biochemistry and molecular biology, **39** (2006), 469–478.

[58] M. Shibuya and L. Claesson-Welsh, *Signal transduction by VEGF receptors in regulation of angiogenesis and lymphangiogenesis*, Experimental cell research, **312** (2006), 549–560.

[59] M. Simeoni, P. Magni, C. Cammia, G. De Nicolao, V. Croci, E. Pesenti, M. Germani, I. Poggesi and M. Rocchetti, *Predictive pharmacokinetic-pharmacodynamic modeling of tumor growth kinetics in xenograft models after administration of anticancer agents*, Cancer Research, **64** (2004), 1094–1101.

[60] H. Takahashi and M. Shibuya, *The vascular endothelial growth factor (VEGF)/VEGF receptor system and its role under physiological and pathological conditions*, Clinical Science, **109** (2005), 227–241.

[61] R. T. Tong, Y. Boucher, S. V. Kozin, F. Winkler, D. J. Hicklin and R. K. Jain, *Vascular normalization by vascular endothelial growth factor receptor 2 blockade induces a pressure gradient across the vasculature and improves drug penetration in tumors*, Cancer research, **64** (2004), 3731–3736.

[62] F. Valeriote and L. van Putten, *Proliferation-dependent cytotoxicity of anticancer agents: a review*, Cancer Research, **35** (1975), 2619–2630.

[63] I. Vivanco and C. L. Sawyers, *The phosphatidylinositol 3-Kinase AKT pathway in human cancer.*, Nature Reviews. Cancer, **2** (2002), 489–501.

[64] Y. Wang, L. Zhang, J. Sagotsky and T. S. Deisboeck, *Simulating non-small cell lung cancer with a multiscale agent-based model*, Theoretical Biology and Medical Modelling, **4** (2007), 50.

[65] Z. Wang, V. Bordas and T. Deisboeck, *Identification of Critical Molecular Components in a Multiscale Cancer Model Based on the Integration of Monte Carlo, Resampling, and ANOVA*, Frontiers in Computational Physiology And Medicine, **2** (2011) .

[66] M. Welter, K. Bartha and H. Rieger, *Emergent vascular network inhomogeneities and resulting blood flow patterns in a growing tumor*, Journal of Theoretical Biology, **250** (2008), 257–280.

[67] C. G. Willett, Y. Boucher, F. Di Tomaso, D. G. Duda, L. L. Munn, R. T. Tong, D. C. Chung, D. V. Sahani, S. P. Kalva, S. V. Kozin, and others, *Direct evidence that the VEGF-specific antibody bevacizumab has antivascular effects in human rectal cancer*, Nature medicine, **10** (2004), 145–147.

[68] F. Winkler, S. V. Kozin, R. T. Tong, S. S. Chae, M. F. Booth, I. Garkavtsev, L. Xu, D. J. Hicklin, D. Fukumura, E. di Tomaso, L. L. Munn and R. K. Jain , *Kinetics of vascular normalization by VEGFR2 blockade governs brain tumor response to radiation Role of oxygenation, angiopoietin-1, and matrix metalloproteinases*, Cancer Cell, **6** (2004), 553–563.

[69] X. Zheng, S. M Wise and V. Cristini, *Nonlinear simulation of tumor necrosis, neovascularization and tissue invasion via an adaptive finite-element/level-set method*, Bulletin of mathematical biology, **67** (2005), 211–259.

Received July 17, 2012; Accepted September 07, 2012.

E-mail address: benjamin.ribba@inria.fr
E-mail address: floriane.lignet@ens-lyon.fr
E-mail address: vincent.calvez@ens-lyon.fr
E-mail address: emmanuel.grenier@ens-lyon.fr